Utrecht University
Institute of Marine and Atmospheric Research

Bachelor Thesis

Modelling the effects of a changing storm climate on characteristics of inner shelf sand ridges

Author:
S.J.M. Boersen

Supervisors:
H.E. de Swart
A. Nnafie

June 29, 2013

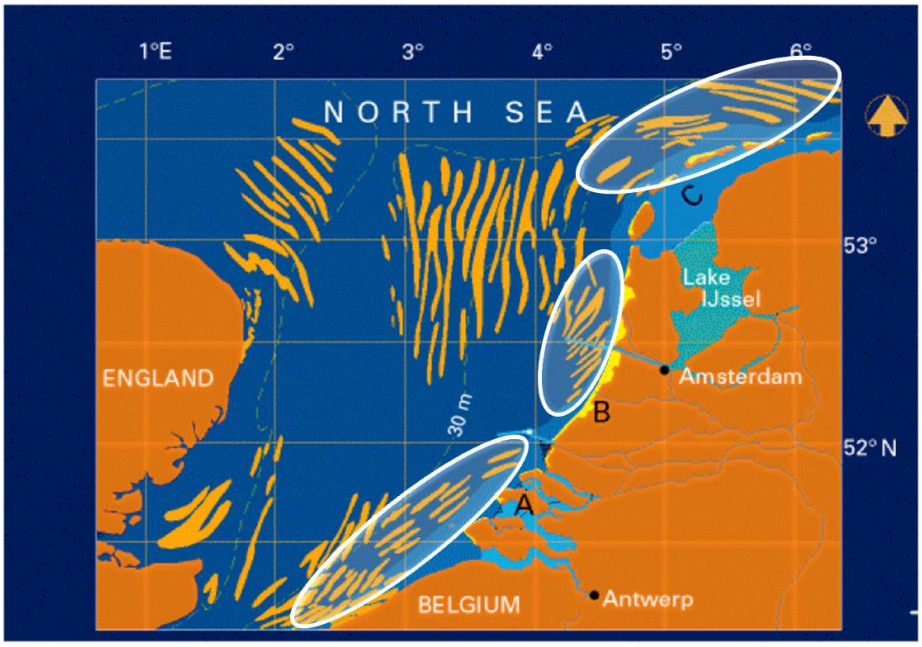

Abstract

A morphodynamical model is used to get further insight in the formation and long time evolution of the large scale bedforms on the inner shelf (circled at the front page). These sand ridges are formed on storm-dominated inner shelves over centeries and weaken the erosion of beaches. Their crest are shifted upstream with respect to where they are attached to the shoreface. Previous studies report constant stormy conditions over the entire formation time. The effects of changing storm climate are studied in this paper. Two changes in storm climate will be investigated: a sudden turn in wind and wave direction and a periodic change of 500 years in wind stress magnitude and offshore wave height. Modelling shows an increase in saturation height after a sudden turn, this is because of the Coriolis term in the shallow water equation. The saturation time after a sudden change is much shorter then when started with random bottom perturbation. Modelling with periodic stormy conditions results in a periodic migration speed and growth of the ridges. The time-averaged height of the ridge is also decreased because of the periodic conditons.

Contents

1 Introduction **3**

2 Model Formulation **4**
2.1 Domain and assumptions 4
2.2 Model structure 5
2.3 Mechanism 6
2.4 Equation of motion 6
2.4.1 Waves 6
2.4.2 Currents 7
2.5 Bathymetry evolution 8

3 Methodology **9**
3.1 Default case 9
3.2 Scenarios 9

4 Model Results **11**

5 Discussion **11**

6 Conclusions **17**

1 Introduction

Approximately 60% of the human populations lives close to shore (Marshak, 2008). The shore gives great opportunities but also brings large risks. The opportunities can be harbours, which provide economic prosperity. One of the main risks that coastal lowlands face, is flooding. Especially the risk of flooding makes modelling and understanding of coastal dynamics systems important.

Inner shelf sand ridges are large-scale undulations of a shore. These ridges can absorb incoming wave energy, which will reduce the erosion of the beach. This will decreases the changes of flooding.

The ridges of interst are formed during stormy conditions over a period of centuries (Calvete and de Swart, 2003). They are observed on inner shelves with a alongshore storm driven current. The key aspect of the formation of the ridges is that they are the most stable mode of a storm dominated inner shelf. The ridges of interest are located at a depths of 10-20 m and have heights of a few meters. They have an upcurrent rotation of 20° - 40° with respect to the coastline (Swift et al., 1978) and migrate several meters per year along the coast. They show a typical asymmetric profile. The downcurrent side of the ridge is much steeper than the upcurrent side (Calvete et al., 2001). An example of the ridges is visible at the Dutch coast (see front picture) and at the Atlantic shelf of North America.

The formation of inner shelf sand ridges was first studied by Trowbridge (1995). He used a linear stability model and showed that patterns resembling ridges could be formed on the inner shelf. Further research was done by Calvete et al. (2001). A spectral model called MORFO25 was used, it showed that ridges with finite height could be modelled. For further investigation a nonlinear model called MORFO56 was developed (Nnafie et al., 2011). It showed that the wave-topography feedback would trap the ridges on the shelf.

All the models mentioned so far assume wind stresses and wave heights which only occure during stroms. These stormy conditions were assumed to be constant over the entire formation time (centuries). The overal objective of this study is to get further insight in the effects of a changing storm climate on the formation and long term evolution of inner shelf sand ridges. The change in storm climate is represented by changes in wind stress and offshore waves.

The field of study is narrowed down into two research question: What are effects of a sudden turn in wind and wave direction on characteristics of inner shelf sand ridges? What is the effect of a periodic change in storm climate on characteristics of inner shelf sand ridges? The characteristics spoken of are the rotation, height, migration and formation time of the sand ridges. To address these question MORFO56 (Nnafie et al., 2011) is going to be used, upgraded with a sinusoidal changing wind stress and wave height.

In section 2 of this report a general overview of the model will be given along with the definition of the domain. This section will also contain the equations of motion and bathymetric evolution. More information about the wind stress, the default parameters for each case and the specific settings of each case are given in section 3. The results are given in section 4, followed by the discussion

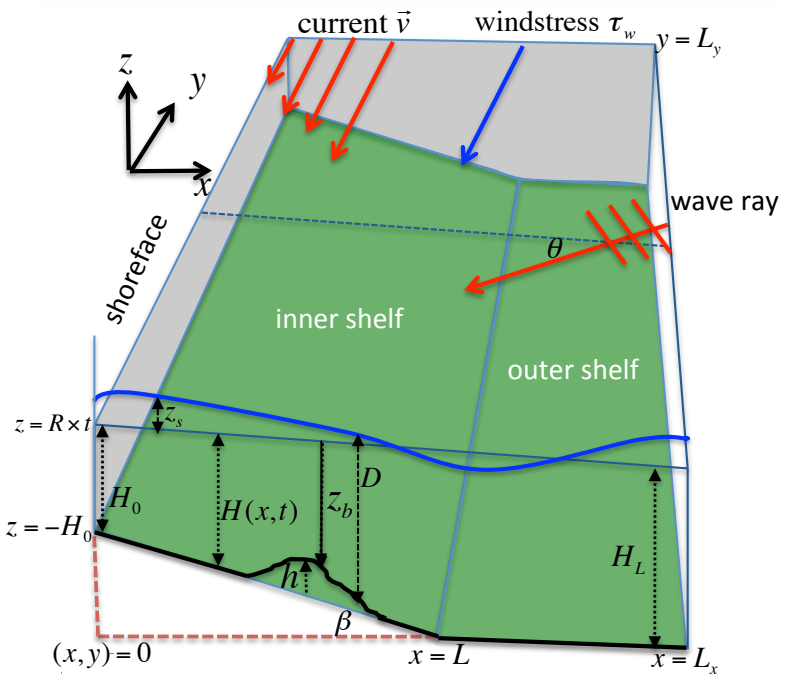

Figure 1: The domain of MORFO56. The explanation and the definition of the symbols is in the text

in section 5. In section 6 the answers on the research questions are given.

2 Model Formulation

2.1 Domain and assumptions

The domain which MORFO56 models is shown in figure 1. In this figure the x is directed cross-shore and y alongshore, z is the position in de vertical. The (depth-averaged) current, windstress and the angle of wave incidence are denoted by: $\vec{v}$, $\vec{\tau_w}$, and θ. Waves are assumed to have a well defined period and angle of incidence. The wave heights are random with a well defined root-mean square (H_{rms}). The domain is divided into a inner- and outer shelf. The outer shelf is defined from $x = L$ until $x = L_x$ with an initial constant water depth of H_L. Water depths are defined with respect to the mean sea level ($z = 0$). The total water depth is given by D and H is the alongshore-averaged water depth. The mean sea level (i.e., averaged over the wave period) has a free surface elevation (z_s). The domain of the inner shelf is defined at $x = 0$ until $x = L$ and has a bottom slope called β. When it is assumed that the slope of the mean

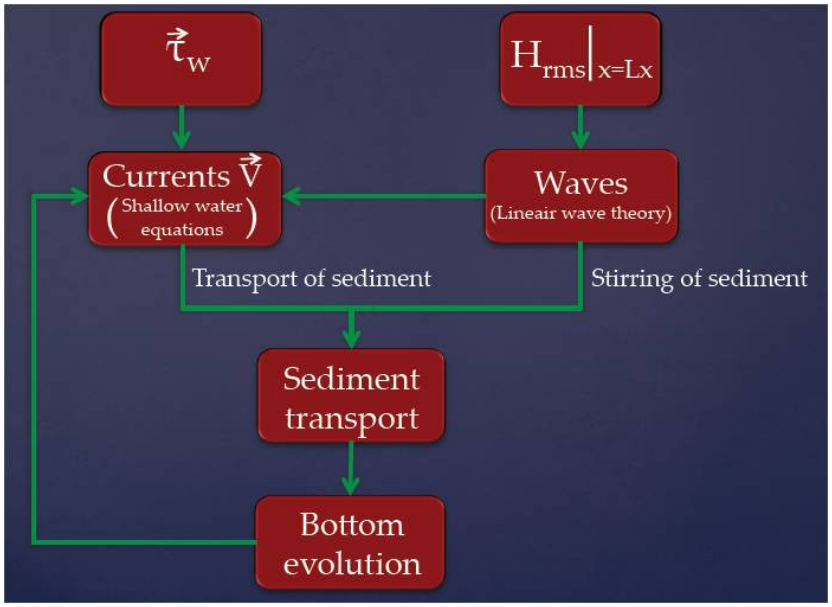

Figure 2: A schematic overview of the structure of MORFO56 (Nnafie et al., 2011), $\vec{\tau}_w$ the wind stress and $H_{rms}\big|_{x=Lx}$ the wave height at the boundary

bottom profile is constant, then the depth profile reads

$$H(x) = \begin{cases} H_0 + \beta x & \text{if } 0 \leq x \leq L, \\ H_L & \text{if } x > L, \end{cases} \tag{1}$$

with H_0 the water depth at the shoreface. The perturbations at the shelf are indicated with h. The bed level with respect to the mean sea level is defined as z_b. At $y = 0$ and $y = L_y$ periodic boundary conditions are used.

2.2 Model structure

The model which is going to be used is MORFO56 created by A. Nnafie. A schematic overview is given in figure 2. The model uses a given wind stress over the entire domain and a constant wave height at the offshore boundary. By linear wave theory the waves are modelled over the entire domain. The wind stress, waves and the bed level result in a current. The waves stir up sediments and the current moves the sediment over the domain. This results in a sediment transport, which results in a bed level evolution. The evolution has effect on the current etc.

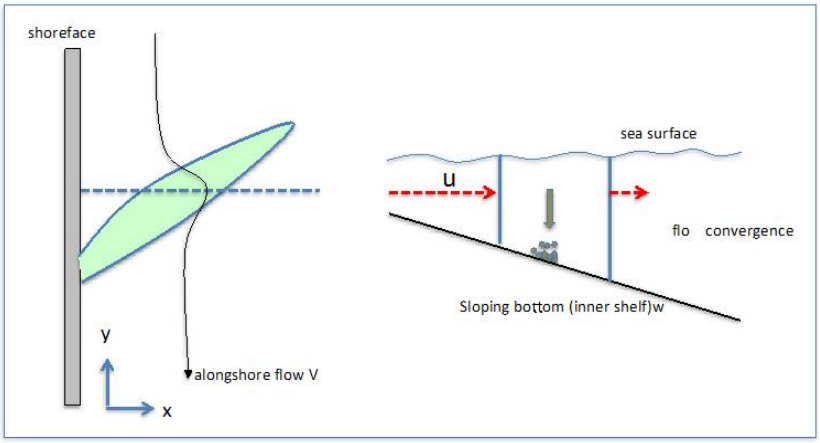

Figure 3: The formations of inner shelf sand ridges. The formation is based on a positive feedback between perturbation and offshore deflection (Trowbridge mechanism) (Trowbridge, 1995)

2.3 Mechanism

The formation of the inner shelf sand ridges is based on a positive feedback between perturbation and offshore deflection. An alongshore flow increases in speed when the depth is decreasing, this is because of the continuity of water. A bed level perturbation can be the reason for a decrease in depth. The increase in speed perpendicular to the perturbation is larger than parallel to the perturbation. This results in a offshore deflection of the current, see figure 3. Because of the sloping bottom of the inner shelf and continuity there will be a decrease in velocity of the current further from the coast. This will lead to a deposition of sediment. This will increase the perturbation size. When the perturbation has a downcurrent rotation the process is the same but only in a decreasing way. A onshore current is developing by which the perturbations shrink.

2.4 Equation of motion

2.4.1 Waves

MORFO 56 uses linear theory to describe the waves (Mei et al., 2005). It uses the conservation of wave crests and the dispersion relation

$$\omega = \sqrt{g\,\kappa \tanh(\kappa D)} = \text{constant}, \tag{2}$$

with ω the wave frequency, g the gravitational acceleration and κ the wavenumber. It also uses the wave number identity relation

$$\frac{\partial}{\partial x}(\kappa \sin\theta) = \frac{\partial}{\partial y}(-\kappa \cos\theta), \tag{3}$$

with θ the wave angle of incidence. The angle θ is chosen positive (negative) clockwise (anti-clockwise). The equations are combined with the wave energy balance

$$\begin{aligned} &\frac{\partial E}{\partial t} + \vec{\nabla} \cdot (\vec{c_g} E) = \mathcal{W} - \varepsilon, \\ &E = \frac{1}{8} \rho \, g \, \mathcal{H}_{rms}^2, \end{aligned} \tag{4}$$

with E the wave energy density, ρ the density of water and $\vec{c}_g$ the group velocity. The amplitude of the group velocity is calculated by

$$c_g = \frac{\omega}{2\kappa} \left(1 + \frac{2\kappa D}{\sinh(2\kappa D)} \right), \tag{5}$$

The first term on the right-hand side of equation 4 is the energy input by the wind. The second term on the right-hand side is the dissipation of energy. There are two mechanisms modelled for this dissipation. The dissipation due to bottom friction (ε_b):

$$\varepsilon_b = \frac{1}{16} \rho c_f \left(\frac{\omega \mathcal{H}_{rms}}{\sinh(\kappa D)} \right)^3, \tag{6}$$

with c_f the drag coefficient. The second mechanism is because of wave breaking (ε_w):

$$\varepsilon_w = \frac{3B^3 \rho g}{32\sqrt{\pi}\gamma_b^2} \frac{\omega \mathcal{H}_{rms}^5}{D^3} \left(1 - \left(1 + (\frac{\mathcal{H}_{rms}}{\gamma_b D})^2 \right)^{-\frac{5}{2}} \right), \tag{7}$$

with γ_b the breakings index and B a breaking coefficient. The total dissipation is the sum of these two. To get an equation for the production of energy in equation 4, it is assumed that there is no net loss or production of energy at x=L. This implies that

$$\mathcal{W} = \varepsilon|_{x=L}. \tag{8}$$

2.4.2 Currents

The currents are described by the depth- and wave-averaged shallow water equations (see Mei et al. (2005) for a derivation)

$$\frac{\partial \vec{v}}{\partial t} + (\vec{v} \cdot \vec{\nabla}) \vec{v} + f \vec{e}_z \times \vec{v} = -g \vec{\nabla}(z_s + s_0 y) + \frac{\vec{\tau}_w}{\rho D} - \frac{\vec{\tau}_b}{\rho D} - \frac{1}{\rho D} \vec{\nabla} \cdot \overline{\overline{S}}, \tag{9}$$

Here f the Coriolis parameter and $\vec{e}_z$ the unit vector in the vertical. The alongshore sea surface gradient is s_0, it contributes to the alongshore flow. Further, $\vec{\tau}_b$ is the bottom shear-stress vector (Nnafie et al., 2011) and $\overline{\overline{S}}$ the radiation

stresses tensor. This term is needed because of the surface gravity waves. These radiation stresses will have effect on the transport of momentum. For a detailed explanation of the radiation stresses see Longuet-Higgins and Stewart (1964). For the exact formulation of the radiation stresses tensor see Nnafie et al. (2011). The bottom shear-stress is modelled by

$$\vec{\tau}_b = \rho r_0 u_{rms} \vec{v}, \tag{10}$$

with r_0 a constant drag coefficient and u_{rms} the root-mean square amplitude of the near-bed wave orbital velocity

$$u_{rms} = \frac{\omega \mathcal{H}_{rms}}{2 \sinh(\kappa D)}. \tag{11}$$

Also a depth integrated continuity equation is going to be used (Mei et al., 2005)

$$\frac{\partial D}{\partial t} + \vec{\nabla} \cdot (D\vec{v}) = 0. \tag{12}$$

2.5 Bathymetry evolution

The sediment transport equations are described by the Bailard's transport formula (Bailard, 1981) with an upgrade to be more valid in stormy conditions (Calvete et al., 2001). The sediment transport during fair weather conditions will be neglected, so it is assumed that the ridges only form during stormy conditions. The sediment transport is dependent on the waves by u_{rms} (stirring) and on the current ($\vec{v}$) (transport). The bed level perturbation is given by

$$(1-p)\frac{\partial h}{\partial t} + \vec{\nabla} \cdot \vec{q} = 0 \tag{13}$$

with $\vec{q}$ the sediment transport and p the porosity. The sediment transport is the sum of the suspended load transport ($\vec{q}_s$) and the bedload transport ($\vec{q}_b$), i.e. $\vec{q} = \vec{q}_b + \vec{q}_s$. Sediments transported in the bedload stay in contact with the bottom. This is different from the suspended load in which the sediments are dissolved in the water and then transported. The bedload transport is modelled by

$$\vec{q}_b = \nu_b (u_{rms}^2 \vec{v} - \lambda_b u_{rms}^3 \vec{\nabla} h), \tag{14}$$

with ν_b a coefficient of the sediment properties and λ a bed slope coefficient. The suspended load is given by

$$\vec{q}_s = \phi \vec{v} - \lambda_s u_{rms}^5 \vec{\nabla} h, \tag{15}$$

with ϕ the volume concentration of sediments and λ_s a slope coefficient. The volume concentration ϕ is wave-averaged and integrated over the depth. Variable ϕ can be physical interpreted as the ratio of volume of sediment particles

in a suspension over the entire water column is used: For the formulation of ϕ the mass balance of suspended sediment is going to be used

$$\frac{\partial \phi}{\partial t} + \nabla \cdot (\phi \, \vec{v}) = w_s(c_a - c_b), \tag{16}$$

with w_s the velocity of the sediment particles, c_a a reference volume concentration and c_b the actual volume concentration near the bed. The first term on the right-hand side models the erosion of sand. In this term the volume concentration is given by

$$c_a = \big(\frac{u_{rms}}{\hat{u}}\big)^3 \tag{17}$$

(Calvete and de Swart, 2003), with $\hat{u}$ calibration velocity to get a realistic concentration for the inner shelf during storms ($\hat{u} \sim 5.0$ ms^{-1}). The second term on the right-hand side of equation 16 represents the sediment deposition. The value of c_b is calculated by

$$c_b = \frac{\phi}{\delta H}\big(1 + \frac{h}{H}\big), \tag{18}$$

with δ the ratio of the characteristic thickness of the suspended load sediment layer and the local water depth D.

The boundary conditions conditions for h are set 0 at $x = 0$ and $x = L_x$. In the along shore direction periodic boundary conditions are used.

3 Methodology

3.1 Default case

The default parameters which are going to be used are based on the Long-Island inner shelf. A domain of 10 km in the cross shore direction (L_x) and 6 km in the along-shore direction (L_y) is used. The calculations make use of a grid with 51 points in the x-direction and 14 points in the y-direction. This results in a grid size of 200 m in the x-direction (Δx) and 430 m in the y-direction (Δy). The random bottom perturbations which are added to the homogeneous domain are of the order of 1 mm. The wind stress ($\vec{\tau_w}$) is directed in the negative y-direction with a (constant) wind magnitude of 0.4 Nm^{-2}. This corresponds to a wind speed of 11 ms^{-1} at a height of 10 m above the sea level. The waves have an angle of incidence of $-20°$ and a wave height at the offshore boundary of 1.5 m. An overview of the default parameters is given in table 1.

3.2 Scenarios

To answer the research questions a default case and 2 scenarios are modelled. Scenario 1 starts exactly the same as the default case but after 5500 years the wind suddenly turns into the direction of the positive y-direction. The wave

	Parameter	Value	Description
hydrodynamics	H_0	$14\,\mathrm{m}$	Depth at shoreface
	H_L	$16.20\,\mathrm{m}$	Depth at outer shelf
	L_x	$10\,\mathrm{km}$	Width of domain
	L_y	$6\,\mathrm{km}$	Length of domain
	β	0.40×10^{-3}	Slope inner shelf
	τ_w	$-0.4\,\mathrm{Nm}^{-2}$	Alongshore wind stress
	r_0	1.87×10^{-3}	Drag coefficient
	s_0	$2 \times 10^{-7}\,\mathrm{m/m}$	Alongshore pressure gradient
	f	$9.3 \times 10^{-5}\,\mathrm{s}^{-1}$	Coriolis parameter
waves	$\mathcal{H}_{rmsc}\|_{x=L_x}$	$1.5\,\mathrm{m}$	Wave height at offshore boundary
	$\theta\|_{x=L_x}$	$-20°$	Wave angle at offshore boundary
	ω	$0.57\,\mathrm{rad\,s}^{-1}$	Wave frequency
	c_f	$3.5 \cdot 10^{-3}$	Wave drag coefficient
	γ_b	0.6	Breaking index
	B	1.0	Breaking coefficient
sediment	ν_b	$3.42 \times 10^{-4}\,\mathrm{s^2m^{-1}}$	Coefficient bedload transport
	λ_b	0.72	Bed slope parameter
	λ_s	$2.06 \times 10^{-2}\,\mathrm{s^4m^{-3}}$	Slope parameter suspended load
	p	0.4	Porosity bottom layer
	$\hat{u}$	$3.66\,\mathrm{ms}^{-1}$	Calibration velocity for erosion
	δ	0.15	Suspended-sediment-layer thickness
	w_s	$0.05\,\mathrm{ms}^{-1}$	Fall velocity of sediment particles
numerics	Δt	0.6 s	Hydrodynamic time step
	Δx	$200\,\mathrm{m}$	Cross-shore grid spacing
	Δy	$430\,\mathrm{m}$	Alongs-shore grid spacing
	α	5000	Morphological amplification factor

Table 1: Default parameter values for currents, waves, bottom topography and numerics

senario	type	$\tau_w(\,\mathrm{Nm}^{-2})$	$H_{rms}\,(\mathrm{m})$	$\theta\,(°)$
default	constant	-0.4	1.5	-20
1	sudden turn in direction	∓ 0.4	1.5	∓ 20
2	periodic magnitude over 500 yrs	$-(0.4 \pm 0.2)$	1.5 ± 0.75	-20

Table 2: Specific settings for each simulation, only parameters which differ from the default case are shown

angle of incidence is switched from $-20°$ to $+20°$. The switch is after 5500 years because then the sand ridge is fully saturated for the current wind stress and wave angle of incidence. Scenario 2 uses a periodic wind stress over the domain and a periodic wave height at the offshore boundary. The wind stress and wave height have a period of 500 years. The wind stress has a average magnitude of $-0.4\,\mathrm{Nm}^{-2}$ and a sinusoidal amplitude of $-0.2\,\mathrm{Nm}^{-2}$ is added. The boundary wave height has an average value of 1.5 m and a sinusoidal height of 0.75 m is added. Tabel 2 gives an overview of these settings.

4 Model Results

In figure 4 the bed level perturbation at different times is shown for the default case. The top left figure shows the random perturbation level at the start, top right panel after 228 years. The two bottom panels are after 1370 and 5251 years. Figure 5 shows the bed level perturbation level for scenario 1. The figures are taken at 5709, 5822, 6050 and 7534 years, so after the sudden change. Different values during the formation process of the sand ridges are shown in figure 6 and figure 7. Panel A shows the ridge height which is defined as the difference between the highest crest and the deepest trough. The growth of the ridges is shown in panel B. It is defined as

$$\sigma = \frac{1}{|h^2|}\frac{\partial}{\partial t}\left(\frac{1}{2}|h^2|\right) \tag{19}$$

(Garnier et al., 2006). The sand ridges migrate over the entire inner shelf. The value for the migration is in panel C. The migration is given by

$$V_m = -\frac{1}{(\partial h/\partial y)^2}\overline{\frac{\partial h}{\partial y}\frac{\partial h}{\partial t}} \tag{20}$$

(Garnier et al., 2006), with the overline the average over the domain is meant. Figure 6, 7 also show the wave height at the offshore boundary (panel D) and the wind stress (panel E).

5 Discussion

Figure 4 shows the bottom perturbation at different times. The panel at the start shows the random bottom perturbation with which each model starts. After 228 years a sorting of the perturbations is already visible. Some perturbations shrink and others grow depending on a positive or negative feedback. The shrinking of the perturbations is also visible in figure 6 panel B. At the start the growth of the ridge is negative. At year 1370 the pattern of the ridge is cleary visible. The ridge covers the entire inner shelf and has an upcurrent rotation. At this point the ridge is still growing. After 5000 years (figure 6 panel A and B) the ridge is fully grown. Comparing the results after 1370 years and 5251 years show that the pattern stays nearly the same and only growth

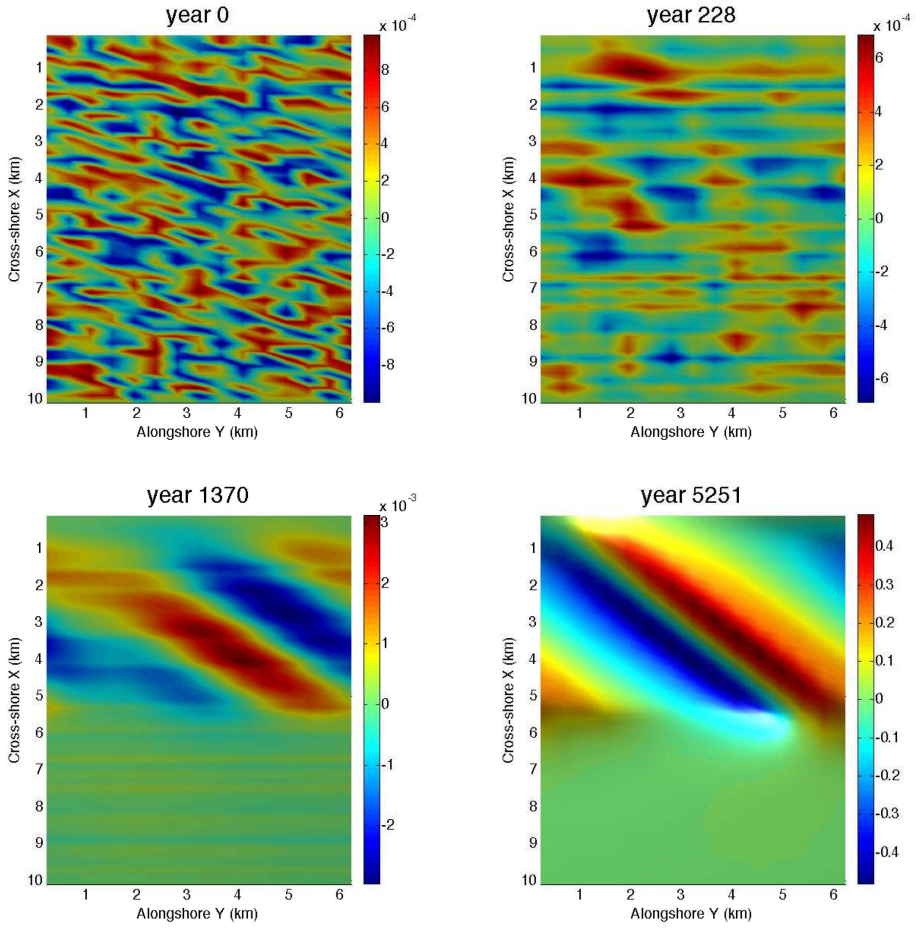

Figure 4: Figures of the perturbation level h in meters at different times of the default case.

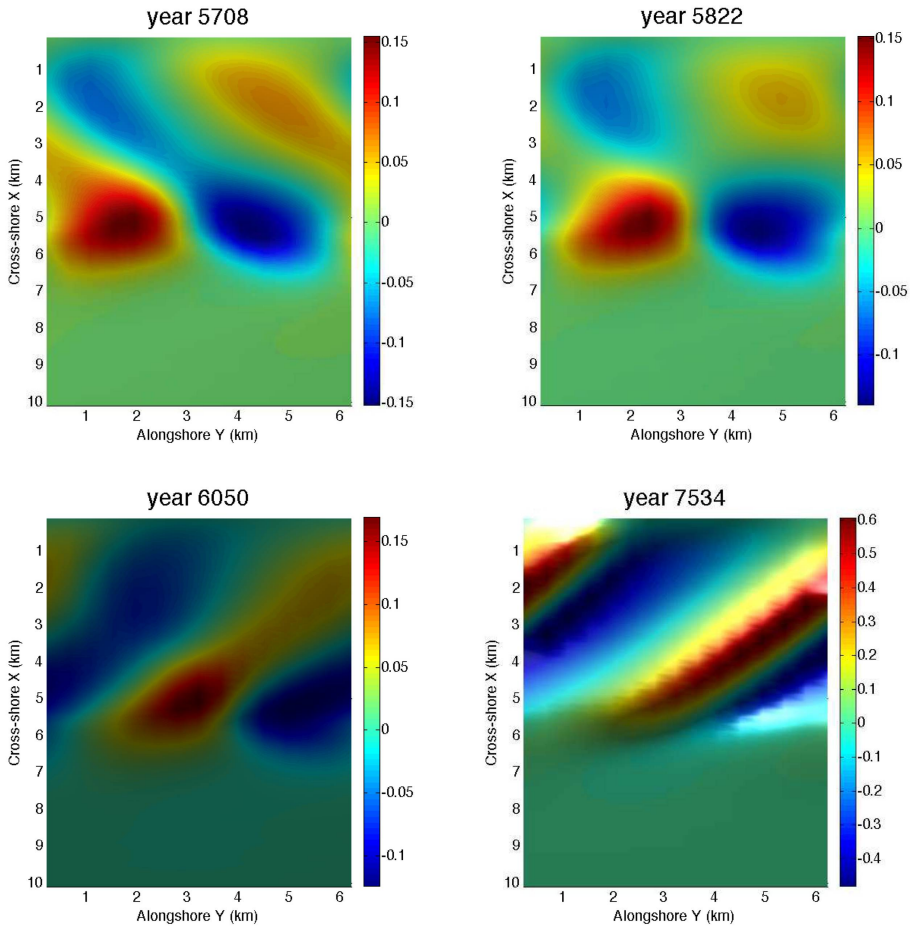

Figure 5: Figures of the perturbation level h in meters at different times of scenario 1.

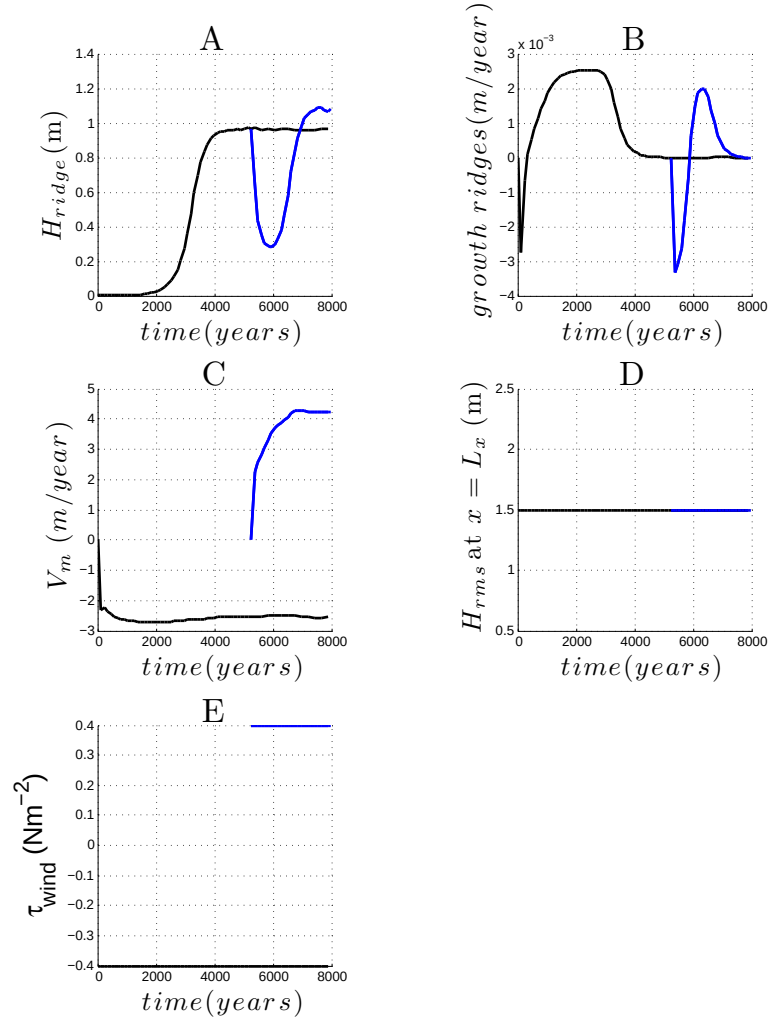

Figure 6: The ridge height (panel A), growth of the ridge (panel B), migrations speed (panel C), incoming wave height at the offshore boundary (panel D) and the wind stress (panel E). The default case is drawn in black and scenario 1 is drawn in blue.

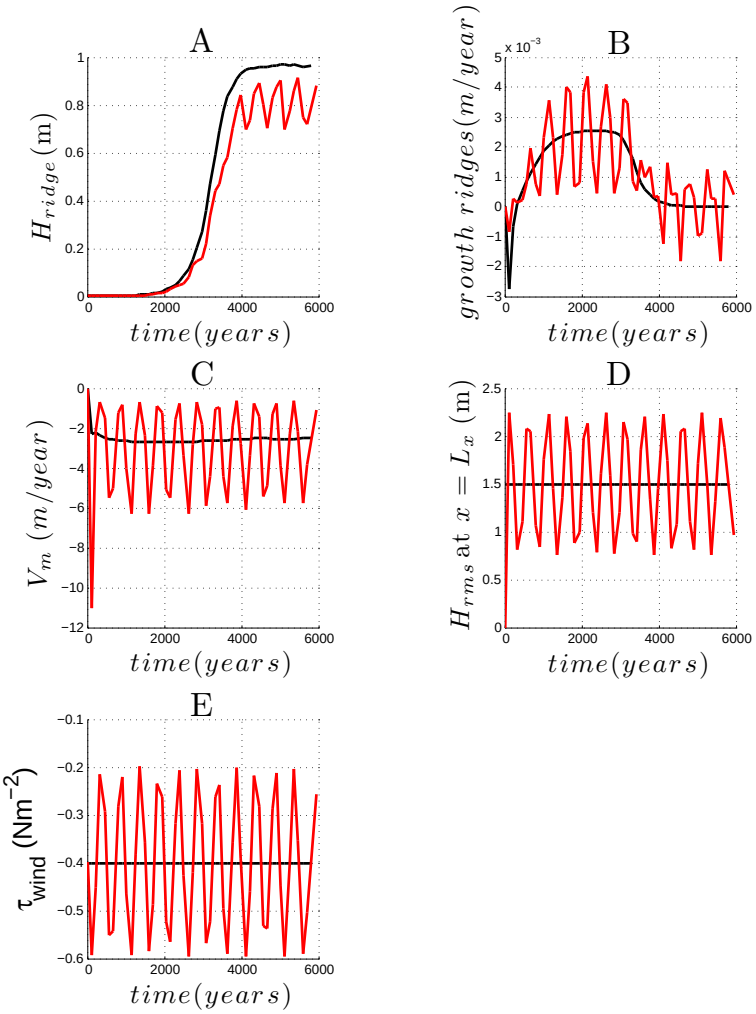

Figure 7: The ridge height (panel A), growth of the ridge (panel B), migrations speed (C), incoming wave height at the offshore boundary (panel D) and the wind stress (panel E). The default case is drawn in black and scenario 2 is drawn in red.

is taking place during this time. Figure 6 panel C shows that the ridge keeps migrating over the entire time also after 5000 years.

The calculations with a sudden turn in wind and wave direction show a large destruction of the ridge during the first 500 years after the turn (see figure 6 panels A and B). The ridge even disconnects from the shoreface (see figure 5). After only 1500 years a new ridge formed and it has reached is maximum height of $\sim 1.1\,\mathrm{m}$. So it takes the ridge much less time to adjust to a sudden change than to build an entire ridge from the start. Taking the Trowbridge mechanism into account explains this phenomenon. A large ridge height results in a larger offshore deflection, which has a positive effect on the growth of the ridge. The already formed ridges can be interpreted as large perturbations. Figure 6 panel A and B support the theory that there is a positive feedback between the ridge height and the migration speed for the dominant ridge wave length.

The change in migration speed after the turn was to be expected because the migration is downcurrent. A change in wind stress direction and wave direction will result in a opposite current. When the ridge keeps migrating downcurrent then the migration speed will also switch sign.

The difference in ridge height between the default case and scenario 1 is a result of the different wind and wave direction, not of the sudden change. Runs which start with a positive wind stress and a positive wave angle of incidence have the same ridge height as the sudden turn scenario. This can be explained by the shallow water equation (equation 9). The equation contains a asymmetric Coriolis term (third term on the left hand-side of equation 9). In the default case the Coriolis term has a negative effect on the ridge height, in scenario 1 a positive. In scenario 1 the offshore deflection of the current is enhanced by the Coriolis term. The difference in absolute value of the migration speed between the default settings and scenario 1 can also be explained by the coriolis term. There is an extra force which has a positive or a negative effect on the ridge characteristics depending on the wind direction.

The effects of a periodic wind stress and wave height are visible in figure 7. In panel A the ridge height of the default case (black) and scenario 2 (red) are shown. For the first 2000 years both cases are nearly the same. A big difference between both scenarios is that the default case saturates after $\sim 4500\,\mathrm{years}$ at a height of $\sim 0.95\,\mathrm{m}$ and that scenario 2 is periodic at this stage. Scenario 2 never saturates but an equilibrium height can be defined of $\sim 0.8\,\mathrm{m}$. The equilibrium level is smaller than the end state of a steady forcing. The growth and migration of the ridges become periodic as well. Panel C shows the migrations speed of both of the cases. The average migrations speed of scenario 2 is $-3.2\,\mathrm{m/year}$. This is more negative than the default case, so the periodicity results in an increase in average migration speed. Panel B of figure 7 shows that the average growth of scenario 2 is smaller than the default case. This is consistent with the ridge height.

6 Conclusions

The objective of the present study was to get further insight in the effects of a changing storm climate on the formation and long term evolution of sand ridges. The study was focused on the effects of a sudden turn in wind and wave direction on characteristics (rotation, saturation time, height and migration speed) of inner shelf sand ridges. The effect of a periodic change in storm climate on characteristics of inner shelf sand ridges was also investigated. These large scale formation form because of sloping bottom which results in a positive feedback between bed level perturbation and sediment deposition. The inner and outer shelf was modelled and showed the formation of sand ridges on the inner shelf.

A default case was examined with a constant wind stress and wave angle of incidence. This was compaired with a scenario which had a sudden change in wind and wave direction when the formed ridges were fully developed. The results show an opposite rotation of the ridge after the sudden change but the rotation is still upcurrent. The saturation time after the sudden change is much shorter than from the start. This is because the inner shelf contains much larger perturbations at this stage. The ridge after the sudden turn had a larger saturation height then previous. This wasn't because of the sudden turn but because of the wind stress and waves from the other direction. After the sudden turn the Coriolis term had a positive effect on the offshore deflection of the current which resulted in a higher saturation height. The migration speed also increased after the sudden turn. This was also not because the sudden turn but because of the opposite direction.

To be able to see what the effect of a periodic change in storm climate on characteristics of inner shelf sand ridges scenario 2 was modelled. It used a sinusoidal wind stress over the entire domain and a sinusoidal wave height at the boundary. The direction of the wind and the wave angle stayed the same during this scenario. The oriention of the ridge stayed the same but difference from the default case is that the ridge never saturated. The ridge height became periodic and had a smaller equilibrium level than the saturation height of the default case. The migration speed became periodic and the mean migration decreased.

References

Bailard, J. A., 1981. An energetics total load sediment transport model for a plane sloping beach. Journal of Geophysical Research 86 (C11), 10938–10.

Calvete, D., Falqués, A., de Swart, H. E., Walgreen, M., 2001. Modelling the formation of shoreface-connected sand ridges on storm-dominated inner shelves. Journal of Fluid Mechanics 441, 169–193.

Calvete, R., de Swart, H. E., 2003. A nonlineair model study on the long-term behavior of shoreface-connected sand ridges. Journal of Geophysical Reserach 108, 3169.

Garnier, R., Calvete, D., Falqués, A., Caballeria, M., 2006. Generation and nonlinear evolution of shore-oblique/transverse sand bars. Journal of Fluid Mechanics 567, 327–360.

Longuet-Higgins, M. S., Stewart, R. W., 1964. Radiation stresses in water wave; a physical discussion, with applications. Deep-Sea Research 11, 529–562.

Marshak, S., 2008. Earth: Portrait of a planet.

Mei, C. C., Stiassnie, M., Dick, K. P. Y., 2005. Theory and Applications of Ocean Surface Waves: Linear Aspects and Nonlinear Aspects. World Scientific.

Nnafie, A., De Swart, H. E., Calvete, D., Garnier, R., 2011. Formation of shoreface-connected sand ridges: effects of rigid-lid approach, quasi-steady approach and wav-topography feedbacks. River, Coastal and Estuarine Morphodynamis: RCEM2011, Tsinghua University Press, Beijing paper D5005.

Swift, D. J. P., Parker, G., Lanfredi, N. W., Perillo, G., Figge, K., 1978. Shoreface-connected sand ridges on American and European shelves: a comparison. Estuarine and Coastal Marine Science 7 (3), 257–273.

Trowbridge, J. H., 1995. A mechanism for the formation and maintenance of shore-oblique sand ridges on storm-dominated shelves. Journal of Geophysical Research 100 (16), 16071–16086.